ADVANCED FUNCTIONAL MATERIALS
www.afm-journal.de

Size-Dependent Staging and Phase Transition in $LiFePO_4/FePO_4$

Changbao Zhu, Lin Gu, Liumin Suo, Jelena Popovic, Hong Li,* Yuichi Ikuhara, and Joachim Maier**

The $LiFePO_4/FePO_4$ phase transition process is remarkable in terms of its excellent reversibility, making this redox system extremely promising for high rate lithium storage. The recent observation of ordering effects ($Li_{0.5}FePO_4$) during the phase transition challenges the traditional two phase models. In this work, the phenomenon of staging for $LiFePO_4$ for different sizes (70 nm and 50 nm) by high resolution aberration corrected annular bright electron microscopy is detected, investigated, and discussed along with previous results on larger crystals. In the small crystals, staging is found throughout with a decrease of order from center to the surface. For the larger crystal, a staging phase occurs constituting the interfacial zone (width around 15 nm) between $LiFePO_4$ and $FePO_4$. A comparison is made to recent experiments on even larger crystals showing such an interphase of smaller extent (around 2 nm). Thus it appears that these zones narrow with increasing size. These findings are discussed in the light of phase transition thermodynamics and kinetics. In particular, the possibility is discussed that the staging interphase may constitute a low energy solution to the $LiFePO_4/FePO_4$ contact.

1. Introduction

The olivine-structured $LiFePO_4$, which was firstly reported by Padhi et al.,[2] as a very promising cathode material and a competitive candidate for electric vehicles, has attracted much attention. In terms of phase transition mechanism, $LiFePO_4$ is widely considered as a typical first-order phase transition material,[2–5] with nucleation and growth of the second phase during phase transition. A variety of models among which core–shell,[2] shrinking core,[3] mosaic,[6] domino-cascade,[7] phase transformation wave,[8] and many particles model[9] are the most prominent, based on the two phase transition mechanism between $LiFePO_4$ and $FePO_4$. For these two phase models, the solid solution single phase materials $Li_{1-y}FePO_4$ and Li_xFePO_4 only exist within very narrow ranges (x, $y < 0.1$) of operation temperature, depending on particle size,[10,11] temperature,[12] and overall composition.[13] The influence of size and interfacial energy on phase stability has been addressed in various papers.[14–18] The phase transition process for large single crystals was found to be diffusion-controlled but resulting in cracks and high porosity owing to the severe volume changes (≈6%).[19] In multiparticle systems, in particular if nanoparticulate, a variety of anomalies have been observed. Delmas et al.[7] observed a digital situation, such that nanoparticles are either fully lithiated or fully delithiated. Gibot et al.[20] reported single phase (de)lithiation for nanoparticles, which has been confirmed by various authors. Sharma et al.[21] found evidence for simultaneous occurrence of solid-solution and two phase reactions through deep discharge of the $Li//LiFePO_4$ cell by real-time in situ neutron powder diffraction. Liu et al.[22] found an intermediate single phase within a limited region in electrochemical delithiated $LiFePO_4$ sample by soft X-ray absorption spectroscopy and theoretical simulations.

Structurally the two phases under concern are extremely similar. From a defect-chemical view point, however, they behave antagonistically.[23] Li sites in $FePO_4$ can be considered as interstitial sites, which when filled are intrinsically compensated by excess electrons (Fe^{2+} instead of Fe^{3+}). For macroscopic crystals interstitial concentrations higher than 8%[11] are thermodynamically not feasible at operation temperature. What can be realized is a situation in which all (or almost all) the Li-sites are filled. The lacking Li-ions must now be viewed as vacancies which are intrinsically compensated by electron holes (Fe^{3+} instead of Fe^{2+}) in $LiFePO_4$ and the concentration of which does not exceed ≈12%.[11] In nanosystems, these narrow solubility ranges are usually not found. This can be attributed to various reasons.

Dr. C. Zhu, Dr. J. Popovic, Prof. J. Maier
Max Planck Institute for Solid State Research
70569, Stuttgart, Germany
E-mail: s.weiglein@fkf.mpg.de
Prof. L. Gu, L. Suo, Prof. H. Li
Beijing National Laboratory for Condensed Matter Physics
Institute of Physics
Chinese Academy of Sciences
Beijing, 100190, China
E-mail: l.gu@iphy.ac.cn; hli@iphy.ac.cn
Y. Ikuhara
WPI Advanced Institute for Materials Research
Tohoku University
Sendai, 980–8577, Japan
Y. Ikuhara
Institute of Engineering Innovation
The University of Tokyo
Tokyo, 113–8654, Japan
Y. Ikuhara
Nanostructures Research Laboratory
Japan Fine Ceramic Center
Nagoya, 456–8587, Japan

DOI: 10.1002/adfm.201301792

© 2013 WILEY-VCH Verlag GmbH & Co. KGaA, Weinheim

According to Malik et al. the excess free energy that intermediate single phase compositions possess, is very small, viz on the order of 5–10 meV per formula unit[24] and may for instance be substantially influenced by capillary contribution.[25] Furthermore, in small crystallites the formation free energy of an interphase might already be costly enough as to avoid local unmixing at the expense of maintaining the macroscopically metastable compositions. Malik et al. stressed the point that in a single phase path the intermediate compositions are quickly passed through. This is due to the non-monotonic dependence of the Li potential on composition and explains why in such cases only end-members are observed. Dreyer et al.[9] showed that the observation that the particles are either fully lithiated or delithiated, is a very consequence of multi-particle thermodynamics irrespective of size. Of course, the rate at which this occurs sensitively depends on size. Clearly, however, in a fully relaxed large single particle situation, phase separation within the particle with an internal interface is thermodynamically expected.[24,26]

With the help of annular-bright-field (ABF) scanning transmission electron microscopy (STEM), light atoms such as lithium can be directly observed at a sub-angstrom resolution.[27] With the help of this advanced methodology, surprisingly a pronounced long-range Li-ordering[28] similar to staging-II structure of graphite[29] intercalation compounds was found expressed by lithium ions occupying every second layer in half delithiated $LiFePO_4$ single-crystalline nanowires[30] corresponding to the composition $Li_{0.5}FePO_4$. In this context, it is worth mentioning that Malik et al.[24] reported on significant short-range ordering found in thermodynamic modeling. In view of the fact that local minima are seen for x_{Li} = 1/6, 2/6, 4/6, 5/6 ordering may be of longer range than reported. Metastable phases with compositions of $Li_{0.75}FePO_4$ and $Li_{0.5}FePO_4$ were obtained by quenching Li_xFePO_4 samples from 400 °C to room temperature.[12] Very recently, a metastable Li_xFePO_4 ($x \approx 0.6$) crystal phase was detected during the electrochemical phase transition process by time-resolved XRD by Orikasa et al.[31] At any rate, a pronounced long-range order (staging structure) challenges the conventional two phase transition mechanism. The complexity is further increased by the recent finding that such a distinct ordering ($Li_{0.5}FePO_4$) was observed in the form of an interphase at the contact of $LiFePO_4$ and $FePO_4$. Again, it was STEM-ABF that revealed this point firstly for Nb-doped $LiFePO_4$ with particle size of ≈200 nm.[1] The interphase is sandwiched between $LiFePO_4$ and $FePO_4$ normal to the c-axis but with more or less curved interfaces. The width of this interfacial zone for this example was reported as being 2 nm. Sun et al. concluded from DFT calculation the $LiFePO_4$/$Li_{0.5}FePO_4$/$FePO_4$ three phase coexistence to correspond to a kinetically controlled thermodynamically metastable state.[26] Table S1 in the Supporting Information summa.rizes various situations mentioned in the literature and the main results in this work.

In order to get a more comprehensive insight, we prepared in this work $LiFePO_4$ nanocrystals the sizes of which (50 nm and 70 nm) were substantially smaller than for the previously reported 200 nm sample. For even tinier particles, the application of ABF unfortunately proved not successful owing to the overlapping of particles. We will give evidence that on partially delithiating $LiFePO_4$ i) the temporal appearance of a thermodynamically or kinetically stable intermediate phase is indeed sensible and ii) the same intermediate phase can also locally play the role of an interphase between $FePO_4$ and $LiFePO_4$.

2. Results and Discussions

70 nm $LiFePO_4$ crystals were prepared by ball-milling commercial carbon-coated $LiFePO_4$. No detectable impurity was found in this sample (see XRD pattern in Figure S1, Supporting Information). **Figure 1** displays an ABF-STEM image of 70 nm $LiFePO_4$ with 10% chemical delithiation viewed from

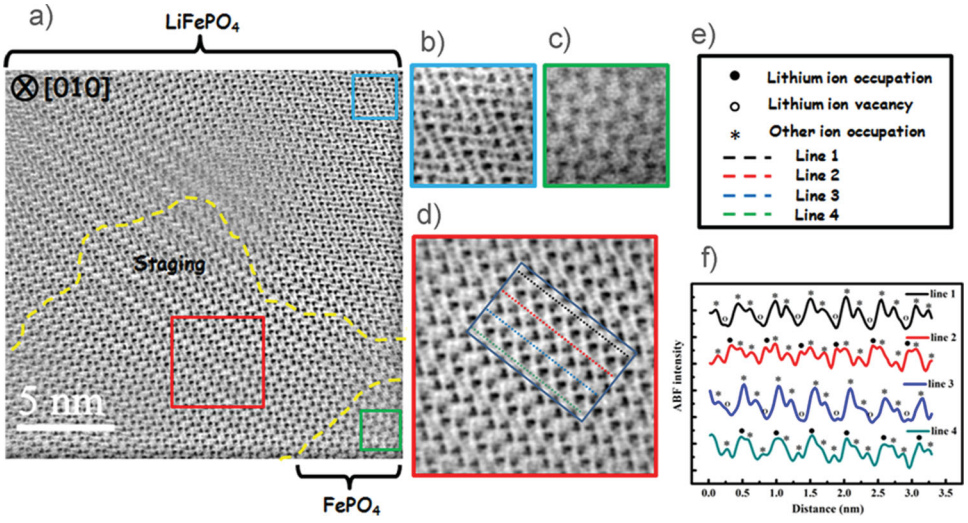

Figure 1. a) ABF-STEM images of 70 nm $LiFePO_4$ viewed at the [010] zone axis. The staging area is marked by the dashed yellow lines. b–d) Enlarged images of $LiFePO_4$ phase, $FePO_4$ phase and interfacial phase with staging structure, corresponding to blue, green and red squares respectively in (a). e,f) the line profiles from the ABF image corresponding to the different colored dashed lines in (d). Note that in the ABF line profile, image contrast of the dark dots is inverted and showed as peaks.

© 2013 WILEY-VCH Verlag GmbH & Co. KGaA, Weinheim

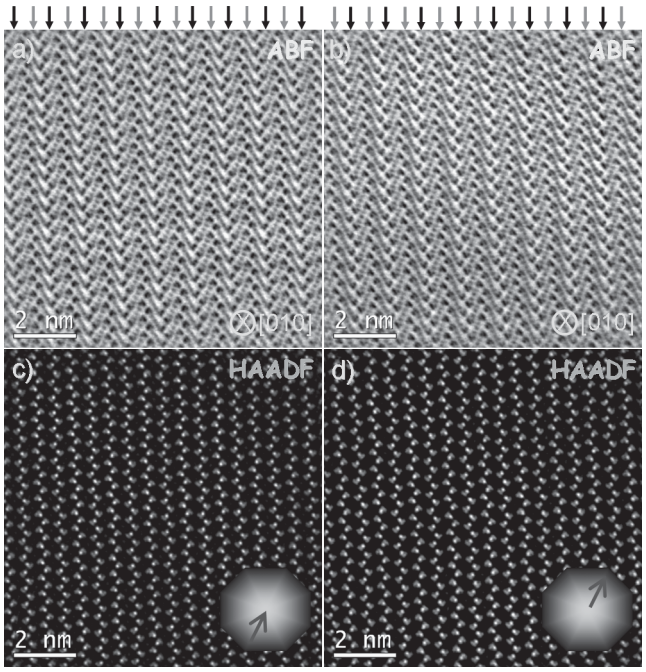

Figure 2. High-angle annular-dark-field (HAADF) and annular-bright-field (ABF) electron images of electrochemically half delithiated carbon-coated 50 nm $LiFePO_4$ viewed at [010] zone axis. The images were acquired at two different areas a,c) from the center of specimen and b,d) from the edge. Orange and cyan arrows indicate atomic rows that have different Li quantity in the projection column. Note that the diffused contrast in the cyan rows strongly implies distortion of the local structure.

[010] orientation. Note that the nonstoichiometric range x for 70 nm $Li_{1-x}FePO_4$ is around 0.035.[11] From both ABF images (Figure 1a) and the significant difference of Li columns intensity in the line profiles (Figure 1f) from three different regions (Figure 1b–d), a staging structure is confirmed forming the interfacial region between $LiFePO_4$ and $FePO_4$ (this is related to as staging II phase elsewhere).[26] Neither morphology nor purity seem to be decisive factors for the appearance of staging, since the ordered structure can be observed in both $LiFePO_4$ nanowires[28] and nanoparticles, as well as in Nb-doped materials. The composition alternates along *a* direction, while the phase boundary is normal to *c* direction. Figure 1 indicates curved rather than planar interphase boundaries.[7] The results are similar to those reported for 10% chemically delithiated Nb-doped 200 nm $LiFePO_4$ sample.[1] A remarkable difference consists in the width of the interphases; for the 70 nm $LiFePO_4$ the width was around 15 nm (the staging structure is marked by yellow dash lines in Figure 1a), while a smaller width of 2nm was detected in 200 nm $LiFePO_4$. Even though there is a scatter in the width observation, the results indicate a distinct variation in the mean value.

To investigate if this trend is pursued at even smaller particles, a carbon-coated 50 nm $LiFePO_4$ was prepared by polyol method[32] with post heat treatment. Phase-pure $LiFePO_4$ was obtained, which is confirmed by XRD (Figure S2). All the peaks can be indexed to orthorhombic olivine $LiFePO_4$ with space group pnma (JCPDS card No. 01–081–1173) without any detectable impurities. Figure S3 (Supporting Information) gives an impression of particle size and size distribution. **Figure 2** shows high-angle annular-dark-field (HAADF) and ABF imaging of an electrochemically half delithiated $LiFePO_4$ particle of 50 nm size viewed from [010] orientation. HAADF and ABF electron images were acquired at two different areas with Figure 2a,c from the center of specimen and Figure 2b,d from the edge. Owing to the relatively poor scattering ability, light atoms, such as O and Li, can not be observed by HAADF images, which delivers only the atomic positions of Fe and P. Hence, similar images are obtained from Figure 2c,d corresponding to the center and edge of the particle. However, the situation is totally different in the ABF images, which reveals not only atomic positions of Fe and P, but also O and Li. Orange and cyan arrows which represent Li occupied sites and delithiation sites respectively in the Figure 2 display clearly a staging structure for both center and edge of the sample. Large area staging appears throughout the whole particle. Note that the diffused contrast in the cyan rows strongly implies distortion of the local structure due to the electrochemical delithiation process. A similar large area staging throughout the entire particle was also observed on electrochemically half-delithiated single-crystalline $LiFePO_4$ nanowire with diameter around 60 nm.[28]

Figure 3 displays line profiles of the ABF images from the center and edge of the specimen, corresponding to Figure 2. The orange and cyan atomic rows exhibit different Li quantities in the projection column, which indicates staging structure.

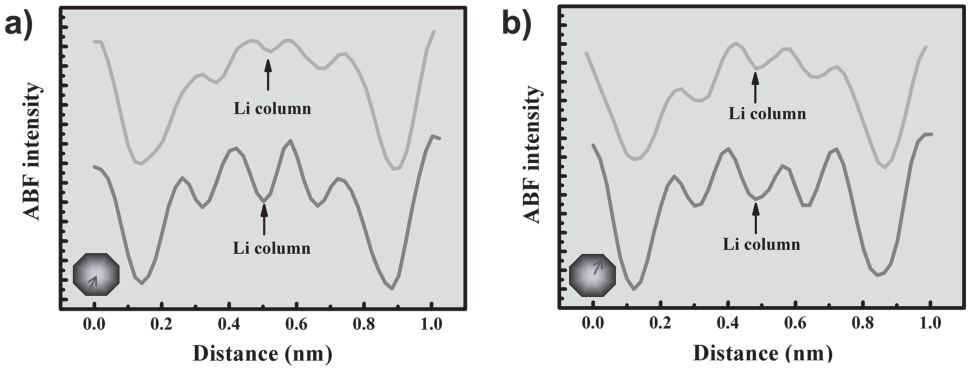

Figure 3. Line profiles of the ABF images from the a) center and b) edge of the specimen. Cyan and orange lines display different Li quantity in the viewing column, which is corresponding to Figure 2.

© 2013 WILEY-VCH Verlag GmbH & Co. KGaA, Weinheim

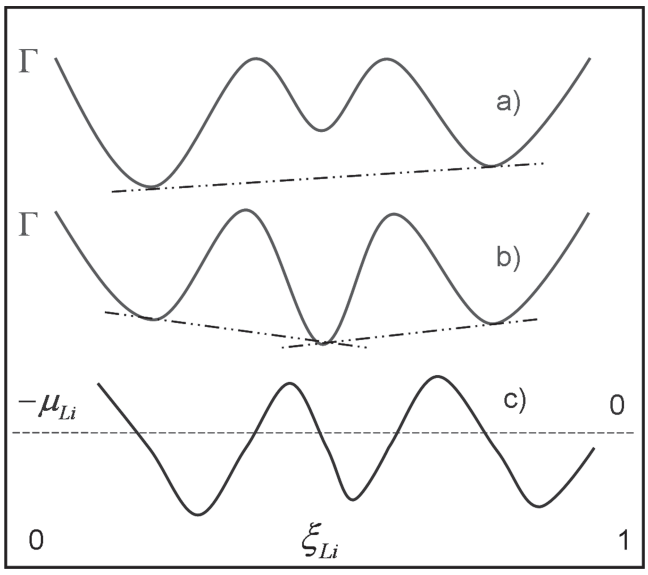

Figure 4. a,b) Different Gibbs free energy curves in the $LiFePO_4/FePO_4$ systems as function of Li content with the existence of low energy staging phase. Note that Γ is the Gibbs energy per number $FePO_4$-units and ξ_{Li} is the ratio of number of Li and number of $FePO_4$. c) The chemical potential of Li, owing to the definition of Γ and ξ_{Li}, as derivative of one above curves.

From the intensity of Li in the orange and cyan rows as well as center and edge lines, decrease of ordering even appears from the center to the edge in one particle. This demonstrates that the staging structure not only appears for the whole particle but also displays gradual variation of the local structure from the center to the edge. The ordering effect is more pronounced in the center of the sample compared to the edge, the easiest explanation would be the symmetry break by the surface weakening long range order. The detailed interpretation for the gradual variation of staging structure in one particle still needs further theoretical investigation.

Let us summarize the major findings. For the small nanoparticles with a nominal composition $Li_{0.5}FePO_4$, we observed a homogeneous staging structure all through the particles. At larger particles with an overall composition of $Li_{0.9}FePO_4$, a $Li_{0.5}FePO_4$ staging structure was found to form an interphase between $LiFePO_4$ and $FePO_4$, the width of which decrease with increasing particle size.

Let us first discuss the homogenous situation. The observation of the $Li_{0.5}FePO_4$ composition throughout could be expression of the extremely sluggish relaxation of such an intermediate metastable composition. The energetic effects connected with this distinctly ordered structure will result in a local minimum in the Gibbs energy as a function of Li-content ($\Gamma(\xi_{Li})$ curves, whereby we denote the Gibbs energy per $FePO_4$ unit by Γ and the Li-content per $FePO_4$ unit by ξ). The corresponding Li-potential ($\mu_{Li}(\xi_{Li})$ curve) is sketched in **Figure 4**c. Applying the same consideration made for the double-minimum in the $\Gamma(\xi_{Li})$ -curve to this case emphasizes the possible role of the $Li_{0.5}FePO_4$ phase as a kinetic attractor. It may even be that–in view of the very small excess values–additional constraints such as capillary, charge, or stress effects make it even a thermodynamic attractor ($Li_{0.5}FePO_4$ as coexisting phase, in Figure 4b).

This would directly explain the very recent detection of an ordered temporal intermediate during the electrochemical charging/discharging process enabled by in-situ time-resolved XRD.[31]

Even more intriguing is the appearance of $Li_{0.5}FePO_4$ as contact phase between $LiFePO_4$ and $FePO_4$. This morphology was observed in the large particle (the overall compositions was fixed to $x = 0.1$). Note that in none of the many investigated regions of all samples, a clean $LiFePO_4/FePO_4$ interface was ever observed in a given particle. This again may be attributed to a very sluggish transient situation, but now expressed in terms of a spatial distribution. This is particularly clear if we refer to a deep minimum as in Figure 4b. Then a non-vanished gradient in the Li-potential would demand such a situation similarly as oxide layer of Fe under a high O_2 partial pressure shows a layer sequence $FeO/Fe_3O_4/Fe_2O_3$.

There is however one point that remains puzzling. Precise determination of the chemical diffusion coefficient of Li in $LiFePO_4$ (D^δ) yielded extrapolated values of 10^{-12} cm^2 s^{-1} at room temperature for large single crystals which are too large for such a sluggish Li-redistribution. Even though D^δ is a complex quantity and not simply given by electronic and ionic mobility values, it is not expected to vary by many orders of magnitude with impurity content. The extrapolated diffusion coefficients at room temperature for $LiFePO_4$, Al-doped $LiFePO_4$ and Si-doped $LiFePO_4$ large single crystals according to the literatures[33–35] are listed in the supporting information (Table S2, Supporting Information). Note that the values already include anti-site defects, which reduce effective transport. It is not expected that the short-range anisotropy will change this conclusion qualitatively. We also do not expect D^δ in $FePO_4$ or in the staging structure to be extremely lower. Again it is pertinent to distinguish between the situations a and b shown in Figure 4. In the first case, it is the $Li_{0.5}FePO_4$ phase that has to disappear if all the gradients in the chemical potential of Li have vanished. Here the requirements for diffusion are minor (small diffusion length). In the second case, the $LiFePO_4$ phase or the $FePO_4$ phase have to disappear if the overall composition is smaller or larger than 0.5 (in our sample we refer to 0.9). In such cases, the diffusion length would be an order of magnitude greater. Let us thus reckon with a diffusion length of 100 nm to be on the safe side. Note that for a 100 nm distance, a diffusion coefficient of 10^{-12} cm^2 s^{-1} would demand a redistribution within 1 min. Redistribution for half a year of waiting time (as relevant here) not to occur would demand a D^δ value of less than 10^{-17} cm^2 s^{-1}. Note that we are also on the safe side if we assume a very small D^δ along c since then D^δ along b would be relevant with particle thickness as effective distance of less than 100 nm. (It is also not intelligible to assume such large transfer resistance for Li at the boundaries as to prevent Li redistribution.) If we exclude such extremely small transport coefficients, we either must assume the unmixing energy to be so extremely close to zero, so that the driving force virtually disappears or we have to seek for an extra thermodynamic argument.

Viewing the staging structure from a crystallographic point of view it appears to be an elegant structure solution for constituting the $LiFePO_4/FePO_4$ interface. (Similar to an ABAB interface forming the junction of AAAA and BBBB.) The volume difference between $LiFePO_4$ and $FePO_4$ is about 6%. Hence for

© 2013 WILEY-VCH Verlag GmbH & Co. KGaA, Weinheim

extended phases one expects an arrangement of misfit dislocations or severe coherency strain. Let us more reasonably assume for the following that $Li_{0.5}FePO_4$ shows a minimum in the $\Gamma(\xi_{Li})$ curve but not so deep that it would thermodynamically be compatible with $LiFePO_4$ or $FePO_4$ (Figure 4a). Then, for the interphase to give rise to a low energy solution, the additional free energy required to form $Li_{0.5}FePO_4$ instead of $LiFePO_4$ and $FePO_4$ must be overcompensated by the free energy gain if the $LiFePO_4/FePO_4$ interface is replaced by the $LiFePO_4/Li_{0.5}FePO_4$ and $Li_{0.5}FePO_4/FePO_4$ interfaces (similar arrangements might apply to an amorphous interface[5]). In a simple elastic model such a gain would indeed be expected. According to Hooke's law, the elastic energy is proportional to the square of the misfit (f). If the prefactors do not vary too much, clearly $2E(f/2) < E(f)$ would result. For extended phases, however, additional higher-dimensional defects are necessary which make the situation less clear. If the misfit is released by a dislocation array, the situation is opposite, provided the material constants do not vary much: for a small angle grain boundary $2E(f/2) > E(f)$ according to Read and Shockley.[36] This is due to the fact that long range elastic dislocation fields dominate the formation energy, and partly compensate on approaching dislocation cores. Since we, however, do not deal with homo-interfaces other contributions may be relevant and the variation of the materials constants may be significant. Beyond that, the charging of dislocations may play an important role. In short, there may be good reasons to consider the possibility that the sum of the two interfacial energies is less than the energy of the $LiFePO_4/FePO_4$ interface.[37] If there is no repulsion of the interfaces, the equilibrium thickness might be very small and much smaller than experimentally observed. Elastic effects (dislocations belonging to different planes) or charging effects may well lead to a repulsion. In **Figure 5** and appendix, a quadratic distance law is exemplarily assumed for the interfacial repulsion (i.e., total interfacial energy decays quadratically with increasing distance) while for not extremely small thicknesses the excess energy of the interphase will increase linearly. As long as the first contribution varies steeply (Figure 5) with details not being decisive, an equilibrium thickness will be established. If now the interaction energy or more reasonably the phase energy might change with size (e.g., through capillary contributions which may be on the orders of a few mV for 50–70 nm), the equilibrium thickness will be even size dependent what could explain the experimental results in greater detail. The appearance of a staging structure seizing the whole particle when size is ≈50 nm or smaller would not automatically be explained by an equilibrium thickness becoming comparable with particle size, because in such a situation, $Li_{0.5}FePO_4$-surfaces would replace the $LiFePO_4/Li_{0.5}FePO_4$ and $Li_{0.5}FePO_4/FePO_4$ interfaces. Yet the explanation can be along those lines since the alternative would imply the formation of a $LiFePO_4/FePO_4$ interface. However, necessary parameters are not yet known to decide if such a model is realistic. What may require further explanation is that the shape of the phase boundaries is found to be irregular. We do not believe that the electron beam plays a significant role in affecting the local structural details, since we did not observe any structural changes during the experiments upon radiation. It is also clear that due to the tiny energetic variations that are of relevance here, a variety of observable situations may be feasible. A more detailed elucidation should be a meritful task of computer simulations.

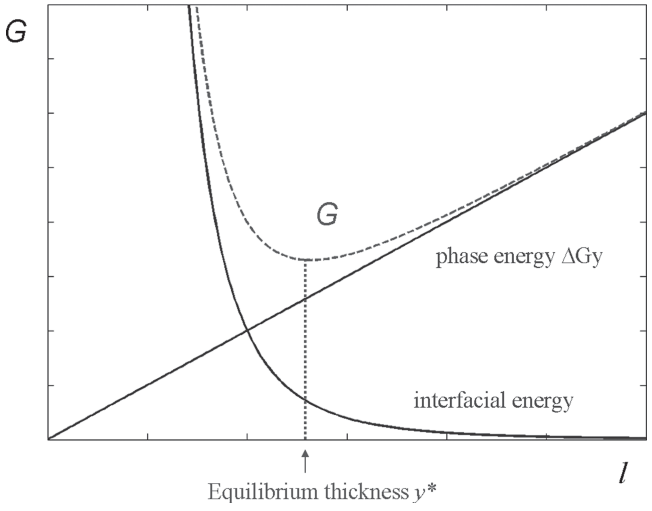

Figure 5. Equilibrium thickness of staging zone from a simple thermodynamic model.

3. Conclusions

In this work, by advanced high resolution ABF-STEM technology, we investigated ordering effects for $LiFePO_4$ particles with different sizes (70 nm and 50 nm) and discussed it together with previous results. Various staging phenomena were observed. For large crystals, staging structures form an intermediate phase between $LiFePO_4$ and $FePO_4$, and the staging interphasial width appears to narrow with increasing size. For small crystals, the staging structure appears throughout the whole particle with decrease of order from center to the surface. The findings are discussed in the light of thermodynamics and kinetics. It seems obvious that the staging phase can form a distinct intermediate between $LiFePO_4$ and $FePO_4$ both in spatial (size-dependent interphase) as well as temporal sense (structural attractor on de/lithiation). These findings are of crucial significance for the understanding of fast charging/discharging behavior of the $LiFePO_4$-$FePO_4$ electrode.

4. Experimental Section

Carbon-coated $LiFePO_4$ with particle size of 50nm was prepared by polyol method with post heat treatment. Li-CH_3COO, Fe-$(CH_3COO)_2$, and $NH_4H_2PO_4$ was dissolved as a stoichiometric equimolar ratio in a tetraethylene glycol (TEG). The solution was heated at 320 °C in a round-bottom flask with magnetic stirring. The flask was attached to a refluxing condenser. The resultant $LiFePO_4$ nanorods were collected by repeated washing and centrifugation with ethanol, acetone three times respectively. Then $LiFePO_4$ powders were dried in a vacuum oven at 80 °C for 20 h. The obtained $LiFePO_4$ powders were dispersed in the D-glucose water solution with magnetic stirring. After evaporated all the water, the $LiFePO_4$/glucose mixture was heated at 700 °C for 12 h in 5% H_2/95% Ar to prepare the carbon-coated $LiFePO_4$ nanoparticles. 70 nm $LiFePO_4$ were prepared by ball milling commercial $LiFePO_4$ (Advanced Lithium Electrochemistry Co., Ltd, Taiwan) under Ar atmosphere.

© 2013 WILEY-VCH Verlag GmbH & Co. KGaA, Weinheim

10% chemical delithiation was carried out for 70 nm $LiFePO_4$. $LiFePO_4$ powders were mixed with proper amount of nitronium tetrafluoro-borate NO_2BF_4 in acetonitrile with magnetic stirring for 24 h at room temperature in the glove box. The product were washed several times with acetonitrile before they were dried under vacuum for 24 h (T = 80 °C). 50% electrochemical delithiation was performed for 50 nm $LiFePO_4$. The charge and discharge cycling was done twice at 0.1 C (10 h to fully charge and discharge), and then the fully charged battery was discharge for 5 h to obtain $Li_{0.5}FePO_4$.

XRD measurements were carried out with a Philips PW 3020 diffractometer using Cu-K_α radiation. Aberration-corrected ABF STEM was performed using a JEOL ARM 200F transmission electron microscope operated at 200 keV. A collection semiangle of 12–25 mrad was used with the illumination semiangle of 25 mrad for the best ABF contrast.[38]

For the electrode preparation, $LiFePO_4$ (70 wt%), carbon black (20 wt%, Super-P, Timcal), and poly(vinylidene fluoride) binder (10 wt%, Aldrich) in N-methylpyrrolidone were mixed. The obtained homogenous slurry was pasted on an Al foil, followed by drying in a vacuum oven at 80 °C for 12 h. Electrochemical test cells (Swagelok-type) were assembled in an argon-filled glove box ($O_2 \leq 0.1$ ppm, $H_2O \leq 3$ ppm) with Al foil covered by active materials as working electrode, lithium metal foil as the counter/reference electrode, and 1 M solution of $LiPF_6$ in a 1:1 vol/vol mixture of ethylene carbonate and diethyl carbonate as the electrolyte (Novolyte technologies). Glass fiber (Whatman) was used as separator. The batteries were charged and discharged galvanostatically in the fixed voltage window between 2.5 V to 4.3 V on an Arbin MSTAT battery tester at room temperature.

5. Appendix

Here, we discuss the possibility of $Li_{0.5}FePO_4$ ($L_{0.5}FP$) to be a stable interphase between $LiFePO_4$ and $FePO_4$ even though exhibiting a higher excess free energy than ½ $LiFePO_4$: ½ $FePO_4$.

I_0: free enthalpy of a $LiFePO_4$ (LFP)/$FePO_4$ (FP) interface

I': free enthalpy of LFP/$L_{0.5}FP$ interface

I'': free enthalpy of FP/$L_{0.5}FP$ interface

x: thickness of LFP region (FP region)

y: thickness of $L_{0.5}FP$ region

We assume planar interfaces.

First assumption is $I^* \equiv I' + I'' < I_0$, (see text)

The second assumption is that I^* decreases with increased thickness of the interphase (see text).

The overall thickness L is:

$L = 2x + y$

Note that this thickness stays constant in a possible transformation process: $L_{0.5}FP \rightarrow \frac{1}{2}LFP + \frac{1}{2}FP$, since $\Delta y = -2\Delta x$ (conservation of PO_4 units).

Owing to the above:

I^* (y=0) = I_0 and $\frac{dI^*}{dy} < 0$

While with increasing y, I^* will decrease, the free enthalpy of the material in between will increase owing to

$$\Delta G_d \equiv \Delta G\{L_{0.5}FP \rightarrow \tfrac{1}{2}LFP + \tfrac{1}{2}FP\} < 0$$

The total free enthalpy is:

$$G = x(G_{LFP} + G_{FP}) + yG_{L_{0.5}FP} + I^*$$

$$G = \frac{L}{2}(G_{LFP} + G_{FP}) + y(-\Delta G_d) + I^*$$

$$\frac{dG}{dy} = -\Delta G_d + \frac{dI^*}{dy}$$

The counteracting behavior leads to interesting consequences. If $I^*(y)$ decreases linearly, we either find no or only staging phase in equilibrium.

(i)

$$I^* = -my + I_0 \text{ and } \frac{dI^*}{dy} = -m \ (m > 0)$$

$$\frac{dG}{dy} = -\Delta G - m = |\Delta G| - |m|$$

If $|m| < |\Delta G| \Rightarrow \frac{dG}{dy} > 0 \Rightarrow$ no intermediate staging phase (y=0).

If $|m| > |\Delta G| \Rightarrow \frac{dG}{dy} < 0 \Rightarrow$ the entire crystallite adopts the staging structure (y=L) (providing surface energy differences are not very significant).

If $|m| = |\Delta G| \Rightarrow$ indifferent (i.e., surface energy difference will be decisive).

If, however, I^* decreases super-linearly, then there will be an equilibrium thickness $0 < y < L$.

Two formal cases are considered: quadratic decrease (ii) and exponential decrease (iii):

(ii)

$$I^* = I_0 - \varepsilon y^2 \left(\text{For } y < \sqrt{\frac{I_0}{\varepsilon}}, \varepsilon > 0\right)$$

$$\frac{dI^*}{dy} = -2\varepsilon y$$

$$\hat{y}^* = \frac{-\Delta G_d}{2\varepsilon} = \frac{|\Delta G_d|}{2\varepsilon}$$

(iii)

$$I^* = I_0 e^{-\alpha y}$$

$$\frac{dI^*}{dy} = -\alpha I_0 e^{-\alpha y}$$

$$\hat{y} = \frac{1}{\alpha}\ln\left(\frac{\alpha I_0}{-\Delta G_d}\right)$$

For the sake of simplicity, case (ii) was chosen for the discussion in the text.

Note that $|\Delta G_d|$ may increase, if y is reduced below the Debye length owing to double layer repulsion.

Supporting Information

Supporting Information is available from the Wiley Online Library or from the author.

Acknowledgement

Discussions with Gerbrand Ceder about short and long range character of metastable compositions and with Wilfried Sigle about dislocations interactions are greatly acknowledged. The authors would like to thanks Gabi Götz for XRD measuremenst, Yongsheng Hu and Yang Sun for helpful discussion. Lin Gu acknowledges the financial support from the "Hundred Talents" program from the Chinese Academy of Sciences and National Natural Science Foundation of China (NSFC) No 11174334. Financial support from CAS innovation project (KJCX2-YW-W26) is also acknowledged.

Received: May 24, 2013
Revised: July 24, 2013
Published online: September 23, 2013

[1] L. M. Suo, W. Z. Han, X. Lu, L. Gu, Y. S. Hu, H. Li, D. F. Chen, L. Q. Chen, S. Tsukimoto, Y. Ikuhara, *Phys. Chem. Chem. Phys.* **2012**, *14*, 5363.

[2] A. K. Padhi, K. S. Nanjundaswamy, J. B. Goodenough, *J. Electrochem. Soc.* **1997**, *144*, 1188.

© 2013 WILEY-VCH Verlag GmbH & Co. KGaA, Weinheim

[3] V. Srinivasan, J. Newman, *J. Electrochem. Soc.* **2004**, *151*, A1517.
[4] L. Laffont, C. Delacourt, P. Gibot, M. Y. Wu, P. Kooyman, C. Masquelier, J. M. Tarascon, *Chem. Mater.* **2006**, *18*, 5520.
[5] G. Y. Chen, X. Y. Song, T. J. Richardson, *Electrochem. Solid-State Lett.* **2006**, *9*, A295.
[6] A. S. Andersson, B. Kalska, L. Haggstrom, J. O. Thomas, *Solid State Ionics* **2000**, *130*, 41.
[7] C. Delmas, M. Maccario, L. Croguennec, F. Le Cras, F. Weill, *Nat. Mater.* **2008**, *7*, 665.
[8] D. Burch, G. Singh, G. Ceder, M. Z. Bazant, in *Theory, Modeling And Numerical Simulation Of Multi-Physics Materials Behavior*, Trans Tech Publications Ltd, Stafa-Zurich, **2008**, pp 95.
[9] W. Dreyer, J. Jamnik, C. Guhlke, R. Huth, J. Moskon, M. Gaberscek, *Nat. Mater.* **2010**, *9*, 448.
[10] N. Meethong, H. Y. S. Huang, W. C. Carter, Y. M. Chiang, *Electrochem. Solid-State Lett.* **2007**, *10*, A134.
[11] G. Kobayashi, S. I. Nishimura, M. S. Park, R. Kanno, M. Yashima, T. Ida, A. Yamada, *Adv. Funct. Mater.* **2009**, *19*, 395.
[12] C. Delacourt, P. Poizot, J. M. Tarascon, C. Masquelier, *Nat. Mater.* **2005**, *4*, 254.
[13] M. Wagemaker, D. P. Singh, W. J. H. Borghols, U. Lafont, L. Haverkate, V. K. Peterson, F. M. Mulder, *J. Am. Chem. Soc.* **2011**, *133*, 10222.
[14] B. B. Straumal, A. A. Mazilkin, S. G. Protasova, P. B. Straumal, A. A. Myatiev, G. Schuetz, E. J. Goering, T. Tietze, B. Baretzky, *Philos. Mag.* **2013**, *93*, 1371.
[15] B. B. Straumal, S. G. Protasova, A. A. Mazilkin, G. Schutz, E. Goering, B. Baretzky, P. B. Straumal, *JETP Lett.* **2013**, *97*, 367.
[16] M. Wagemaker, F. M. Mulder, A. Van der Ven, *Adv. Mater.* **2009**, *21*, 2703.
[17] A. Van der Ven, M. Wagemaker, *Electrochem. Commun.* **2009**, *11*, 881.
[18] L. Wang, F. Zhou, Y. S. Meng, G. Ceder, *Phys. Rev. B* **2007**, *76*.
[19] K. Weichert, W. Sigle, P. A. van Aken, J. Jamnik, C. Zhu, R. Amin, T. Acarturk, U. Starke, J. Maier, *J. Am. Chem. Soc.* **2012**, *134*, 2988.
[20] P. Gibot, M. Casas-Cabanas, L. Laffont, S. Levasseur, P. Carlach, S. Hamelet, J. M. Tarascon, C. Masquelier, *Nat. Mater.* **2008**, *7*, 741.
[21] N. Sharma, X. W. Guo, G. D. Du, Z. P. Guo, J. Z. Wang, Z. X. Wang, V. K. Peterson, *J. Am. Chem. Soc.* **2012**, *134*, 7867.
[22] X. Liu, J. Liu, R. Qiao, Y. Yu, H. Li, L. Suo, Y.-s. Hu, Y.-D. Chuang, G. Shu, F. Chou, T.-C. Weng, D. Nordlund, D. Sokaras, Y. J. Wang, H. Lin, B. Barbiellini, A. Bansil, X. Song, Z. Liu, S. Yan, G. Liu, S. Qiao, T. J. Richardson, D. Prendergast, Z. Hussain, F. M. F. de Groot, W. Yang, *J. Am. Chem. Soc.* **2012**, *134*, 13708.
[23] C. Zhu, K. Weichert, J. Maier, *Adv. Funct. Mater.* **2011**, *21*, 1917.
[24] R. Malik, F. Zhou, G. Ceder, *Nat. Mater.* **2011**, *10*, 587.
[25] J. Jamnik, J. Maier, *Phys. Chem. Chem. Phys.* **2003**, *5*, 5215.
[26] Y. Sun, X. Lu, R. Xiao, H. Li, X. Huang, *Chem. Mater.* **2012**, *24*, 4693.
[27] X. He, L. Gu, C. Zhu, Y. Yu, C. Li, Y.-S. Hu, H. Li, S. Tsukimoto, J. Maier, Y. Ikuhara, X. Duan, *Mater. Express* **2011**, *1*, 43.
[28] L. Gu, C. Zhu, H. Li, Y. Yu, C. Li, S. Tsukimoto, J. Maier, Y. Ikuhara, *J. Am. Chem. Soc.* **2011**, *133*, 4661.
[29] J. E. Fischer, T. E. Thompson, *Phys. Today* **1978**, *31*, 36.
[30] C. Zhu, Y. Yu, L. Gu, K. Weichert, J. Maier, *Angew. Chem. Int. Ed.* **2011**, *50*, 6278.
[31] Y. Orikasa, T. Maeda, Y. Koyama, H. Murayama, K. Fukuda, H. Tanida, H. Arai, E. Matsubara, Y. Uchimoto, Z. Ogumi, *J. Am. Chem. Soc.* **2013**, *135*, 5497.
[32] D.-H. Kim, J. Kim, *Electrochem. Solid-State Lett.* **2006**, *9*, A439.
[33] R. Amin, J. Maier, P. Balaya, D. P. Chen, C. T. Lin, *Solid State Ionics* **2008**, *179*, 1683.
[34] R. Amin, C. T. Lin, J. Maier, *Phys. Chem. Chem. Phys.* **2008**, *10*, 3524.
[35] R. Amin, C. T. Lin, J. B. Peng, K. Weichert, T. Acarturk, U. Starke, J. Maier, *Adv. Funct. Mater.* **2009**, *19*, 1697.
[36] W. T. Read, W. Shockley, *Phys. Rev.* **1950**, *78*, 275.
[37] W. Sigle, C. Sarbu, D. Brunner, M. Rühle, *Philos. Mag.* **2006**, *86*, 4809.
[38] S. D. Findlay, N. R. Lugg, N. Shibata, L. J. Allen, Y. Ikuhara, *Ultramicroscopy* **2011**, *111*, 1144.

© 2013 WILEY-VCH Verlag GmbH & Co. KGaA, Weinheim